*Estudios Geográficos*
85 (296), enero-junio 2024, e155
ISSN-L: 0014-1496 | eISSN: 1988-8546
https://doi.org/10.3989/estgeogr.2024161.161

ARTÍCULOS / *ARTICLES*

# Discrimination of geological units in southern margin of Alborz Mountain in Iran using ASTER satellite imagery

**Komeil Rokni**
Gonbad Kavous University, Golestan, Iran
rokni@gonbad.ac.ir
ORCID ID: https://0000-0003-4238-4017

**Davood Akbari**
University of Zabol, Zabol, Iran
davoodakbari@uoz.ac.ir
ORCID ID: https://0000-0001-8617-8093

Recibido: 25/09/2022; Aceptado: 02/08/2023; Publicado: 04/10/2024

**Cómo citar este artículo/citation: Rokni, Komeil & Akbari, Davood (2024).** Discrimination of geological units in southern margin of Alborz Mountain in Iran using ASTER satellite imagery, *Estudios Geográficos*, 85 (296), e155. https://doi.org/10.3989/estgeogr.2024161.161

**Abstract**: In this study, the effectiveness of several image processing techniques, including the band ratio (BR), decorrelation stretch (DS), principal components analysis (PCA), minimum noise fraction (MNF), as well as the ASTER false color composition RGB: 468, was evaluated for the extraction of geological units from ASTER satellite imagery in southern margin of Alborz Mountain in Iran. In addition, a method based on Principal Components of Band Ratios (BRs-PCs) was proposed for discrimination of geological units from ASTER imagery. In this respect, a scene of ASTER Level1T VNIR+SWIR data of the year 2004 was acquired, and a geological map scale 1:100000 of the study area was used as the reference. The results indicated suitability of the conventional image processing techniques for discrimination of geological units, especially the PCA technique, which clearly highlighted Limestone, Basalt, Sandstone, Tuff, Conglomerate, and Dolomite from the ASTER image. The study also demonstrated effectiveness of the BRs-PCs method for geological mapping. This approach considered the advantages of both PCA and BR techniques, therefore, provided a superior result comparing to any of these techniques alone, and also better result comparing to other techniques used in this study. Thus, it may be useful for geological mapping along the whole Alborz Mountain with similar lithological and geomorphological conditions.

**Keywords**: ASTER imagery; Alborz Mountain; Geological mapping; BRs-PCs

## Discriminación de unidades geológicas en el margen sur de la montaña Alborz en Irán utilizando imágenes de satélite ASTER

**Resumen**: En este estudio, la efectividad de varias técnicas de procesamiento de imágenes, incluida la band ratio (BR), decorrelation stretch (DS), principal components analysis (PCA), minimum noise fraction (MNF), así como la composición de color falso ASTER RGB: 468, fue evaluada para la extracción de unidades geológicas a partir de imágenes de satélite ASTER en el margen sur de los montes Alborz en Irán. Además, se propuso un método basado en componentes principales de proporciones de bandas (BRs-PCs) para la discriminación de unidades geológicas a partir de imágenes ASTER. En este sentido, se utilizó un escenario de datos ASTER Level1T VNIR+SWIR del año 2004 y como referencia un mapa geológico escala 1:100000 del área de estudio. Los resultados indicaron la idoneidad de las técnicas convencionales de procesamiento de imágenes para la discriminación de unidades geológicas, especialmente la técnica PCA, que destacó claramente la piedra caliza, el basalto, la arenisca, la toba, el conglomerado y la dolomita de la imagen ASTER. El estudio también demostró la eficacia del método BRs-PCs para el mapeo geológico. Este enfoque consideró las ventajas de las técnicas PCA y BR, por lo tanto, proporcionó un resultado superior en comparación con cualquiera de estas técnicas solas, y también un mejor resultado en comparación con otras técnicas utilizadas en este estudio. Por lo tanto, puede ser útil para el mapeo geológico a lo largo de toda la montaña Alborz con condiciones litológicas y geomorfológicas similares.

**Palabras clave**: imaginería ASTER; Montaña de Alborz; Mapeo geológico; BR-PC

## 1. INTRODUCTION

Geological mapping is the process of physically going to the field observation and recording the geological information from the rocks that protrudes from the surface of the earth. The information that usually the scientists attempt to find are the boundaries between different structures and rock types, such as fault-lines and evidence of the rocks undergoing deformation (Davis et al., 2011). Geologic mapping is a scientific field that aims to produce usable maps for various applications, such as quality assessment of ground waters and pollution hazards; land-use planning and land management; forecasting volcano, landslide, and earthquake; describing energy and mineral resources as well as their extraction costs; waste repository location; and general education (Compton, 1985; Soller, 2002). A powerful tool that can be implemented to improve the process of geological mapping is the technology of remote sensing (Varnes, 1974; Bernknopf, 1993; Pour and Hashim, 2015; Yang et al., 2018).

Remote sensing technology is useful for the explorations of minerals and geothermal energy, geological investigations, and assessment of geotechnical engineering and environmental geology. Remote sensing is also an essential tool for understanding the significant natural hazards pertinent to geology such as earthquakes, floods, avalanches, river channel migration and avulsion, liquefaction, landslides and debris flows, sinkholes, subsidence, tsunamis, and volcanoes (Bhan and Krishnanunni, 1983). The modern and applicable remote sensing tools include optical images, thermal data, LiDAR and digital elevation models (DEM), microwave and SAR data, hyperspectral remote sensing, and archived aerial photos and satellite images. Therefore, it is possible to perceive the Earth beyond our visual capability and transact the temporal and spatial limitations of earth observations (Prost, 2013).

Many image processing techniques have been presented in recent decades for purposes of geological mapping using remote sensing technology, such as band ratio (Inzana et al., 2003), correlation coefficient (Kühn et al., 2009), principal component analysis (Loughlin, 1991), optimum index factor (Fal et al., 2019), decorrelation stretch (Kenea, 1997), and log residual (Hook et al., 1992), etc. In this study, the applicability of different image processing techniques including the band ratio, decorrelation stretch, principal components analysis, and minimum noise fraction, as well as false color composition ASTER RGB:468 was investigated for discrimination of different geological units from ASTER Level1T VNIR+SWIR data.

The effectiveness of Terra Advanced Spaceborne Thermal Emission and Reflection Radiometer (ASTER) satellite data for lithological mapping and discrimination of geological units was demonstrated in many studies during the recent decades (Hewson et al., 2005; Pournamdari et al., 2014; Abdelouhed et al., 2022). The suitability of ASTER image for geological applications is mainly due to the spectral characteristics of the ASTER visible/near-infrared (VNIR), shortwave infrared (SWIR), and thermal infrared (TIR) bands, consequently, possibilities to perform different image processing techniques for mapping geological units (Rokni et al., 2011; Hewson et al., 2017; Rezaei et al., 2020).

## 2. MATERIALS AND METHODS

### 2.1 Study area

The test site is located in northeastern Iran in Semnan province. The region is surrounded by the mountains and foothills of the North Alborz Mountains which belongs to the Alp-Himalaya orogenic belt. The active morphodynamics in this region are mainly driven by aeolian and fluvial activities. The fluvial activities are prominent as slop deposits, alluvial domains and mega fans (Ullmann et al., 2016). This region is covered by concrete layers such as cretaceous formations, as well as sandstone and paleogene-related conglomerates (Arabameri et al., 2019). Figure 1 shows location of the study area.

### 2.2 Dataset

To carry out discrimination of geological units in the study area, one scene of the ASTER L1T collection acquired in August 2004 was obtained from the US Geological Survey (USGS) Global Visualization Viewer. ASTER Level 1 Precision Terrain Corrected Registered At-Sensor Radiance (AST_L1T) data contains calibrated at-sensor radiance, which corresponds with the ASTER Level 1B (AST_L1B), that has been geometrically corrected, and rotated to a north-up UTM projection. The bands available in the AST_L1T include three Visible and Near Infrared (VNIR) bands, six Shortwave Infrared (SWIR) bands, and five Thermal Infrared (TIR) bands (NASA, 2021). Specifications of the ASTER data is presented in Table 1.

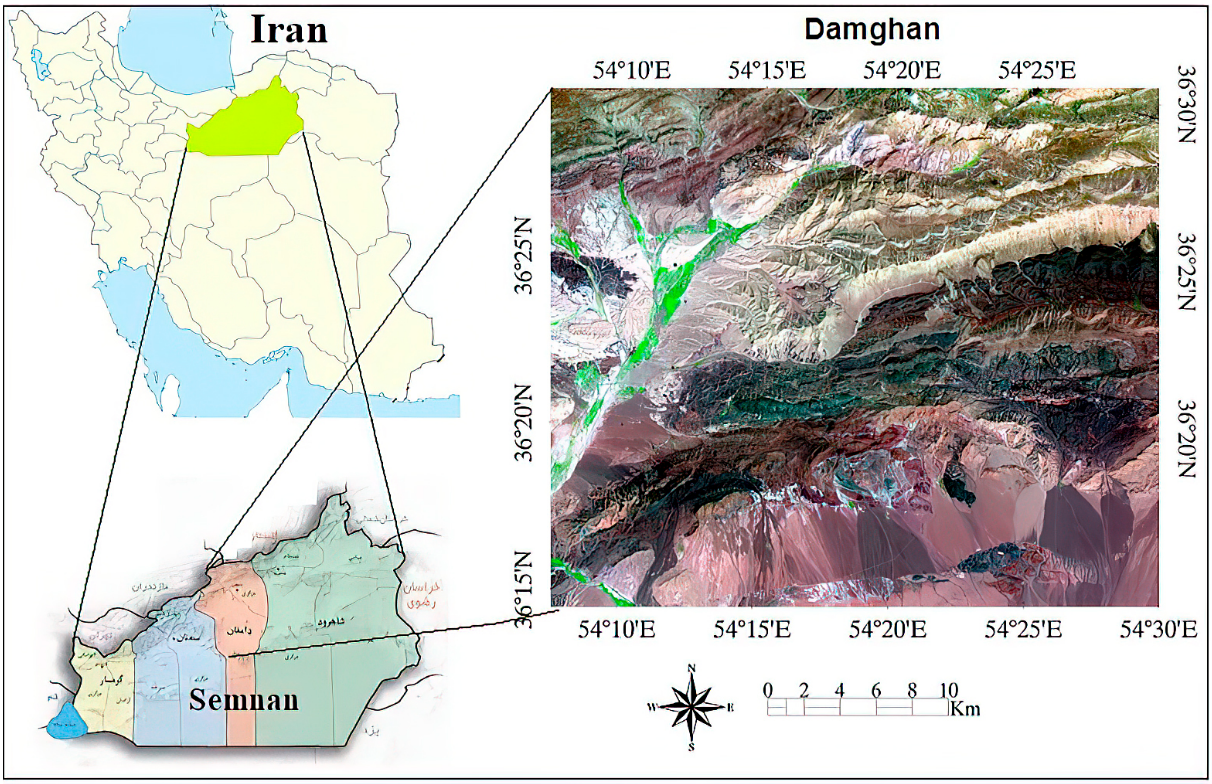


Figure 1. Location of the study area

Table 1. Specifications of Aster image used in this study

| Satellite | Sensor | Year | Band | Description |
|---|---|---|---|---|
| ASTER | TERRA | 2004 | VNIR_Band1 | 15 meter resolution VNIR Band 1(0.52 to 0.60 µm) |
| | | | VNIR_Band2 | 15 meter resolution VNIR Band 2 (0.63 to 0.69 µm) |
| | | | VNIR_Band3N | 15 meter resolution VNIR Band 3N (0.78 to 0.86 µm) |
| | | | SWIR_Band4 | 30 meter resolution SWIR Band 4 (1.600 to 1.700 µm) |
| | | | SWIR_Band5 | 30 meter resolution SWIR Band 5 (2.145 to 2.185 µm) |
| | | | SWIR_Band6 | 30 meter resolution SWIR Band 6 (2.185 to 2.225 µm) |
| | | | SWIR_Band7 | 30 meter resolution SWIR Band 7 (2.235 to 2.285 µm) |
| | | | SWIR_Band8 | 30 meter resolution SWIR Band 8 (2.295 to 2.365 µm) |
| | | | SWIR_Band9 | 30 meter resolution SWIR Band 9 (2.360 to 2.430 µm) |

### 2.3 Geological mapping techniques

The applicability of several image processing techniques including the band ratio (BR), decorrelation stretch (DS), principal components analysis (PCA), minimum noise fraction (MNF), and principal components analysis of band ratios (BRs-PCs) was investigated for discrimination of different geological units in the study area from ASTER satellite imagery. Before applying the specified techniques, the false color composition ASTER RGB: 468, which is generally suitable for geological mapping, was tested for this purpose.

Band ratio is a useful technique for geological studies to extract spectral features that are not observable in the raw bands. This technique use to reduce the topographic variations and differences in image brightness associated with size variable (Adams and Felic, 1967; Sultan et al., 1986). Band ratio is useful for lithological mapping, specially to discriminate rock units in ophiolite complexes (Ninomiya et al., 2005; Amer et al., 2010; Gabr et al., 2010). Several band rations that have previously been verified for geological purposes were evaluated, and consequently the ASTER band ratios (4/1, 4/5, 4/6) = (SWIR-B4/VNIR-B1, SWIR-B4/SWIR-B5, SWIR-B4/SWIR-B6) were found more suitable for detailed lithological mapping in the study area.

Another technique which was used for geological mapping is decorrelation stretch. This technique is useful to remove high correlation that commonly found in multispectral images and is also appropriate to generate a more colorful composite image for the purpose of visualization and to improve image interpretation (Gillespie et al., 1998). Decorrelation stretch was widely used for ophiolite mapping in previous studies (Kenea, 1997; Khan et al., 2007; Seleem et al., 2020).

A standard PCA transformation was applied to ASTER image in this study. This technique was applied on ASTER VNIR+SWIR bands due to suitability of these bands to extract geological units (Aali et al., 2022; Pournamdari et al., 2014). A total of nine new principal components were created from the VNIR and SWIR bands of ASTER image. The first three PCs (PC1, PC2, and PC3) that contains 97.78 percent of total variance (in which the first principal component (PC1) accounts for 84.65%, PC2 accounts for 11.97% and PC3 accounts for 1.16% of the total variance) were used for geological mapping in this study.

Minimum noise fraction is a noise reduction process that usually uses to increase the signal-to-noise ratio in multispectral data. The algorithm of MNF consists of two consecutive rotations of PCA. The first rotation uses the noise covariance matrix to decorrelate and resize the noise in the satellite image. The second rotation uses the PCs which were derived from the outcome of the first rotation. The data space is divided into two parts. One part is associated with large eigenvalues and coherent eigen images and another part with near-unity eigenvalues and noise-dominated images (Green et al., 1988).

The BRs-PCs approach is based on principal component analysis of band ratios. To perform this method, the selected band ratios that was found appropriate for geological mapping in present study, were calculated from the ASTER image. Subsequently, the obtained band ratios were stacked into one composite file. The principal component analysis (PCA) technique was then applied to transform the achieved composite image into a new PCA space. Finally, the resulting principal components of the band rations (BRs-PC1, BRs-PC2, BRs-PC3 as RGB) were evaluated for geological mapping.

### 2.4 Reference map

A geological map scale 1:100000 was used as the reference to evaluate the effectiveness of the applied image processing techniques for discrimination of different geological units in the study area from ASTER imagery. This geological map is displayed in Figure 2.

## 3. RESULTS AND DISCUSSION

At first, an evaluation on false color composition (RGB: 468) of ASTER image was implemented. With reference to the geology map of the study area (Figure 2), our inspection indicated that some of the geological units such as Basalt, Tuff, Conglomerate, and Dolomite can be discriminated from the ASTER RGB: 468 color composition, as shown in Figures 3.

Subsequently, the band ratio, decorrelation stretch, principal components analysis, and minimum noise fraction techniques were applied to find out their applicability in highlighting different geological units from ASTER imagery. Several band rations that have previously been verified for geological purposes were examined and consequently the ASTER band ratios (4/1, 4/5, 4/6) was found more suitable for detailed lithological mapping in the study area. As displayed in Figure 4, the ASTER band ratios (4/1, 4/5, 4/6) clearly discriminated Dolomite, Tuff, Sandstone, Conglomerate, and specially Basalt from the ASTER data. Besides, the outcome of decorrelation stretch demonstrated greatly discrimination of Limestone, Basalt, Tuff, Conglomerate, and Dolomite from ASTER image (Figure 5). This technique was able to highlight all the geological units in the study area except for Sandstone.

PCA technique also was applied on ASTER image (figure 6). Based on statistical analysis and also percentage of data variation, the results showed that the first PC involved the highest variance with positive loadings at each band. PC1 can extract information about lithological and mineralogical rock units through visual interpretations. The last two PCs include small

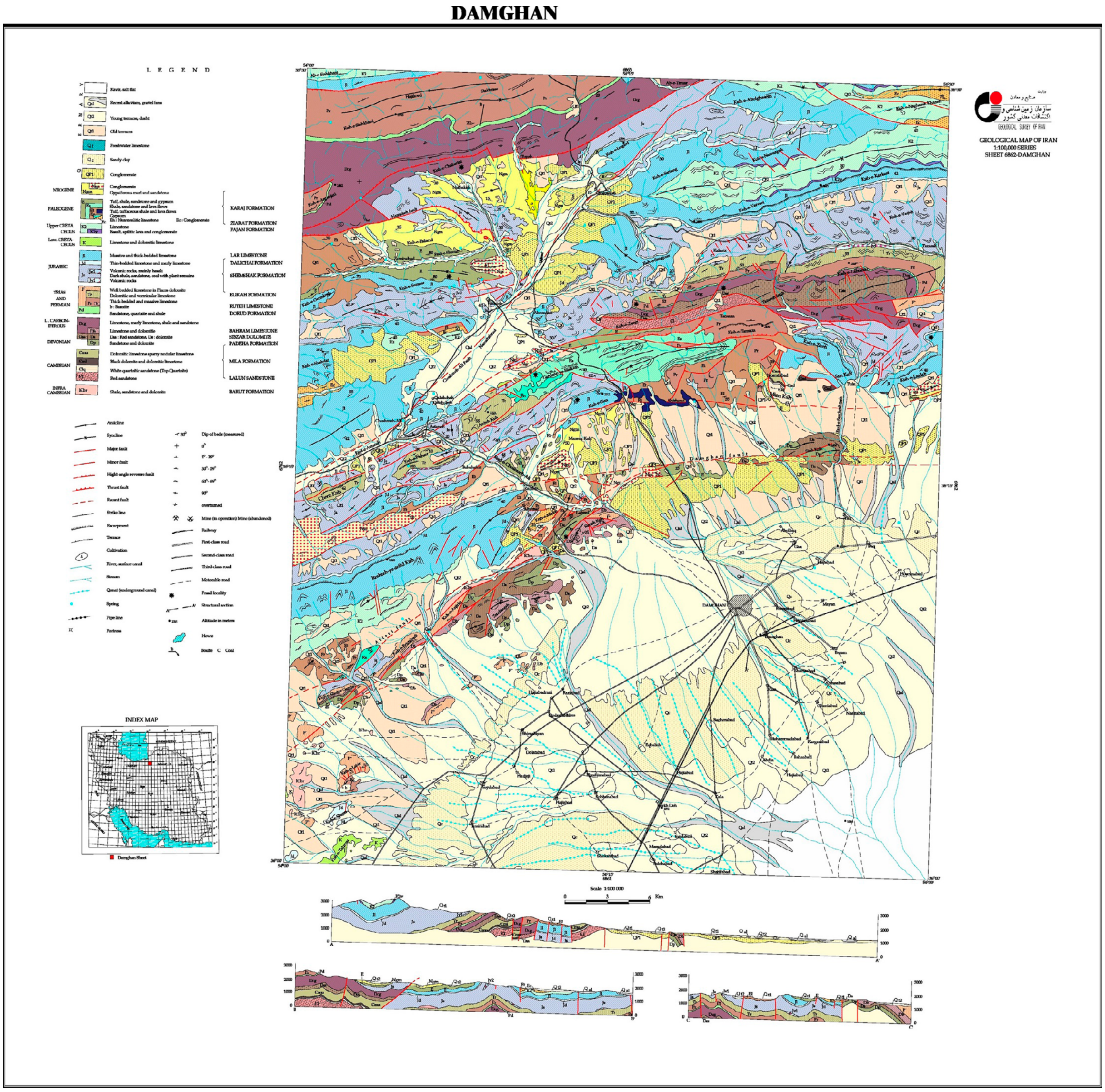


Figure 2. Geological map of Damghan city (covering the study area)

variance with mostly noise. Therefore, the band combination PC1PC2PC3 that contains about 97.78 percent of total variance was selected. Our investigation revealed that the PCA technique is suitable to discriminate Tuff, Limestone, Basalt, Sandstone, Dolomite, and Conglomerate. However, some Basalt units that were adjacent to Sandstone were not differentiated by this technique.

MNF technique was implemented to highlight lithological units from ASTER imagery, as illustrated in Figure 7. The result show that MNF approach is suitable to highlight Basalt, Tuff, Dolomite, and some areas containing Conglomerate, while it is difficult to discriminate Sandstone and Limestone using this technique.

Finally, the BRs-PCs method was performed on ASTER imagery of the study area and the output image was evaluated to assess the applicability of this method to highlight geological units. In doing so, the PCA technique was applied on the selected band ratios in this study (4/1, 4/5, 4/6 as RGB), and the obtained PCs (BRs-PC1, BRs-PC2, BRs-PC3 as RGB)

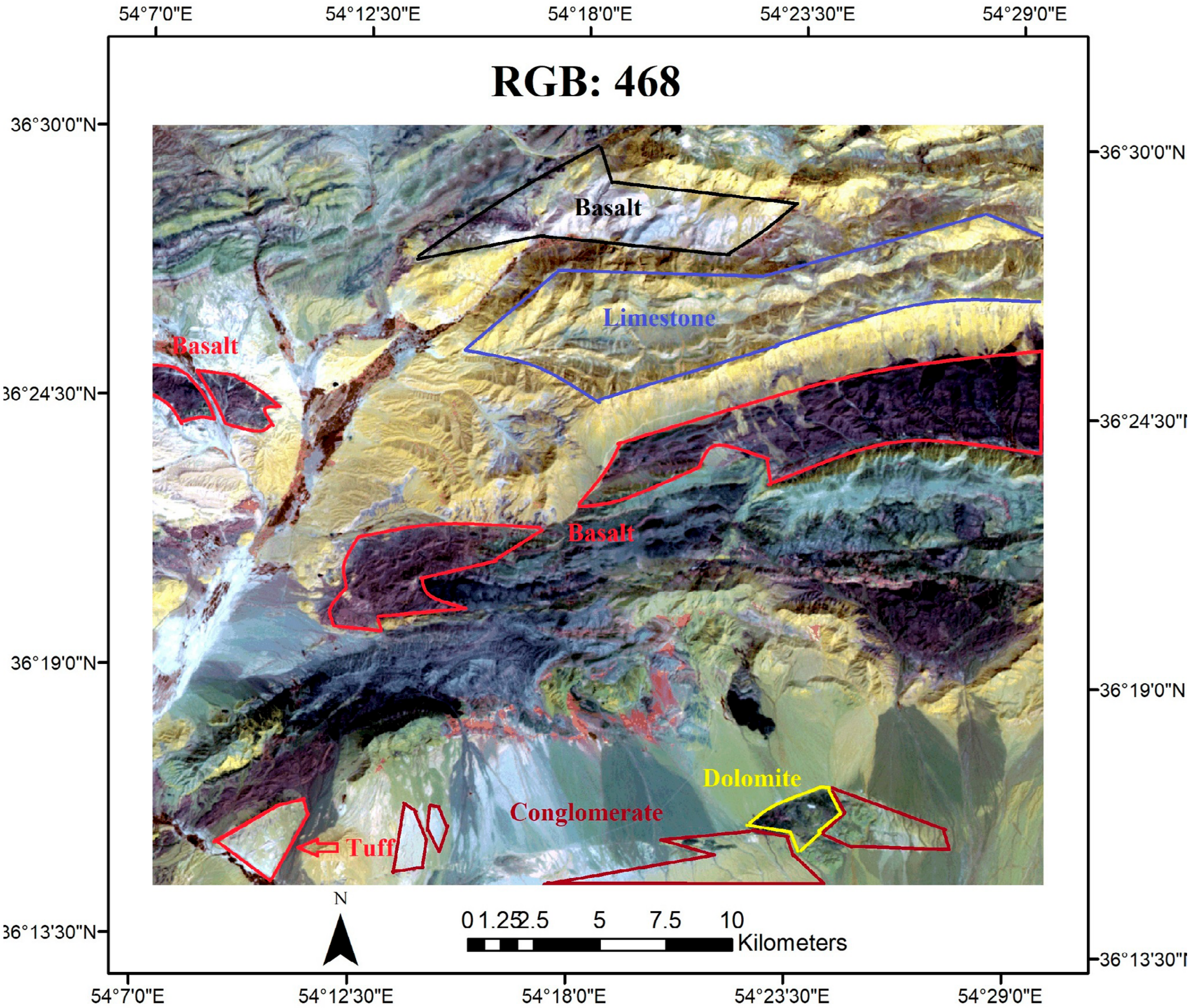


Figure 3. False color composition (RGB: 468) of ASTER image

were analyzed. The result demonstrated the effectiveness of BRs-PCs method for geological mapping. As displayed in Figure 8, this approach provided an enhanced output compared to methods PCA and BR alone, and clearly discriminated the available geological units in the study area.

Overall, as presented in Table 2, the findings of this study indicate that discrimination of Conglomerate, Tuff, Dolomite, and Basalt units from ASTER image at the region of Alborz Mountain was easy, so that all the applied techniques were able to clearly extract these geological units. On the other hand, discrimination of Limestone and Sandstone was difficult and these geological units were not identified by some of the applied techniques. The ASTER band combination 468 that is well known for geological mapping, was also not able to discriminate Limestone and Sandstone.

The specified band ratios could not extract Limestone from ASTER image. In contrast, although PCA technique highlighted all the geological units in the study area, but some errors was appeared in extraction of Basalt using this technique. But BRs-PCs approach, because considered the advantages of both PCA and BR techniques, provided a superior output compared to PCA and BR methods alone, and also better result compared to other applied techniques in this study. The BRs-PCs approach successfully discriminated all the geological units from ASTER imagery.

The findings of this study were confirmed by the results of previous studies in different regions. In

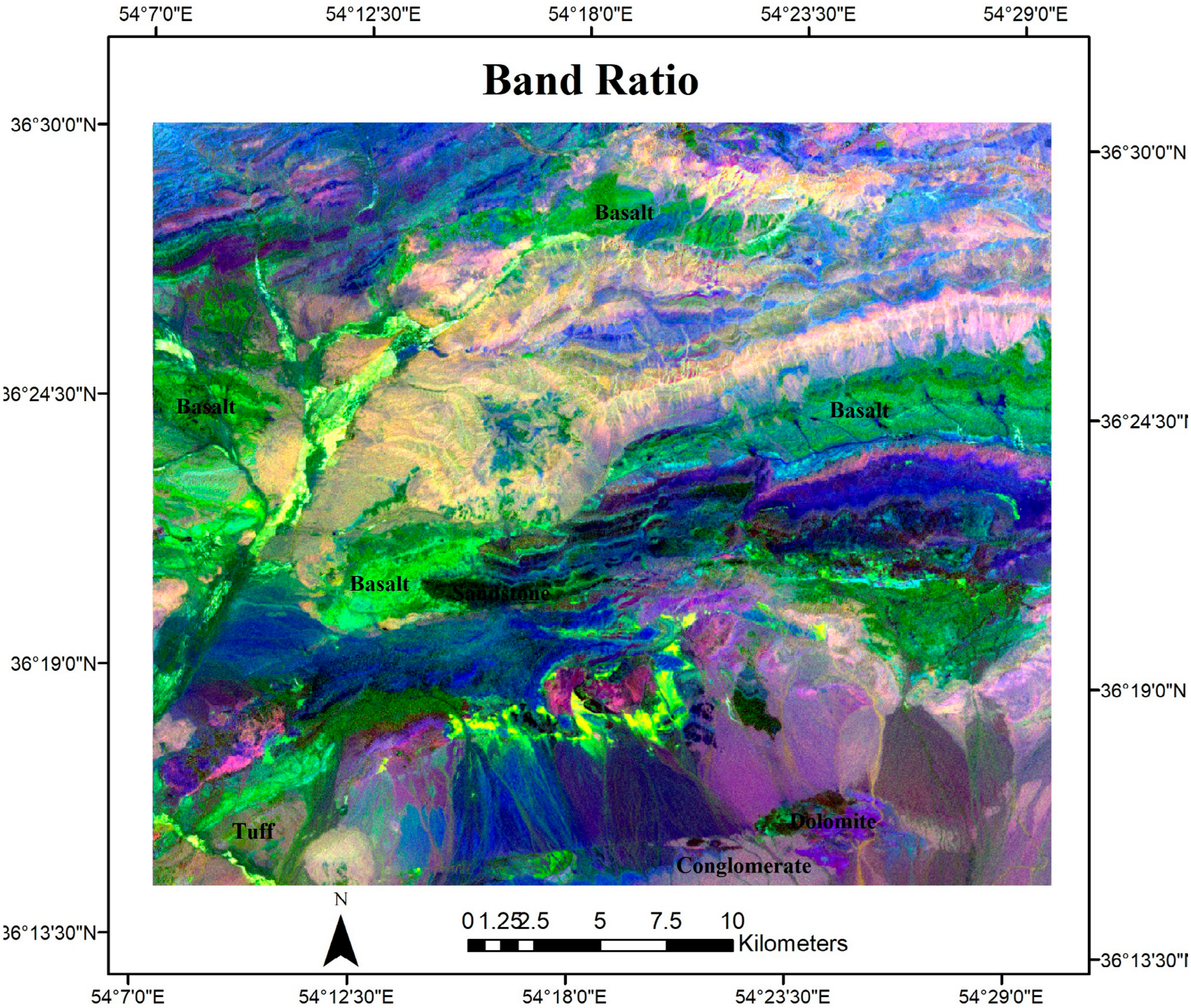


Figure 4. Band ratios (4/1, 4/5, 4/6 as RGB)

Table 2. Suitability of the applied techniques for geological mapping (Y=Yes and N=No)

| | Conglomerate | Limestone | Sandstone | Dolomite | Basalt | Tuff |
|---|---|---|---|---|---|---|
| **RGB: 468** | Y | N | N | Y | Y | Y |
| **BR** | Y | N | Y | Y | Y | Y |
| **DS** | Y | Y | N | Y | Y | Y |
| **PCA** | Y | Y | Y | Y | Y | Y |
| **MNF** | Y | N | N | Y | Y | Y |
| **BRs-PCs** | Y | Y | Y | Y | Y | Y |

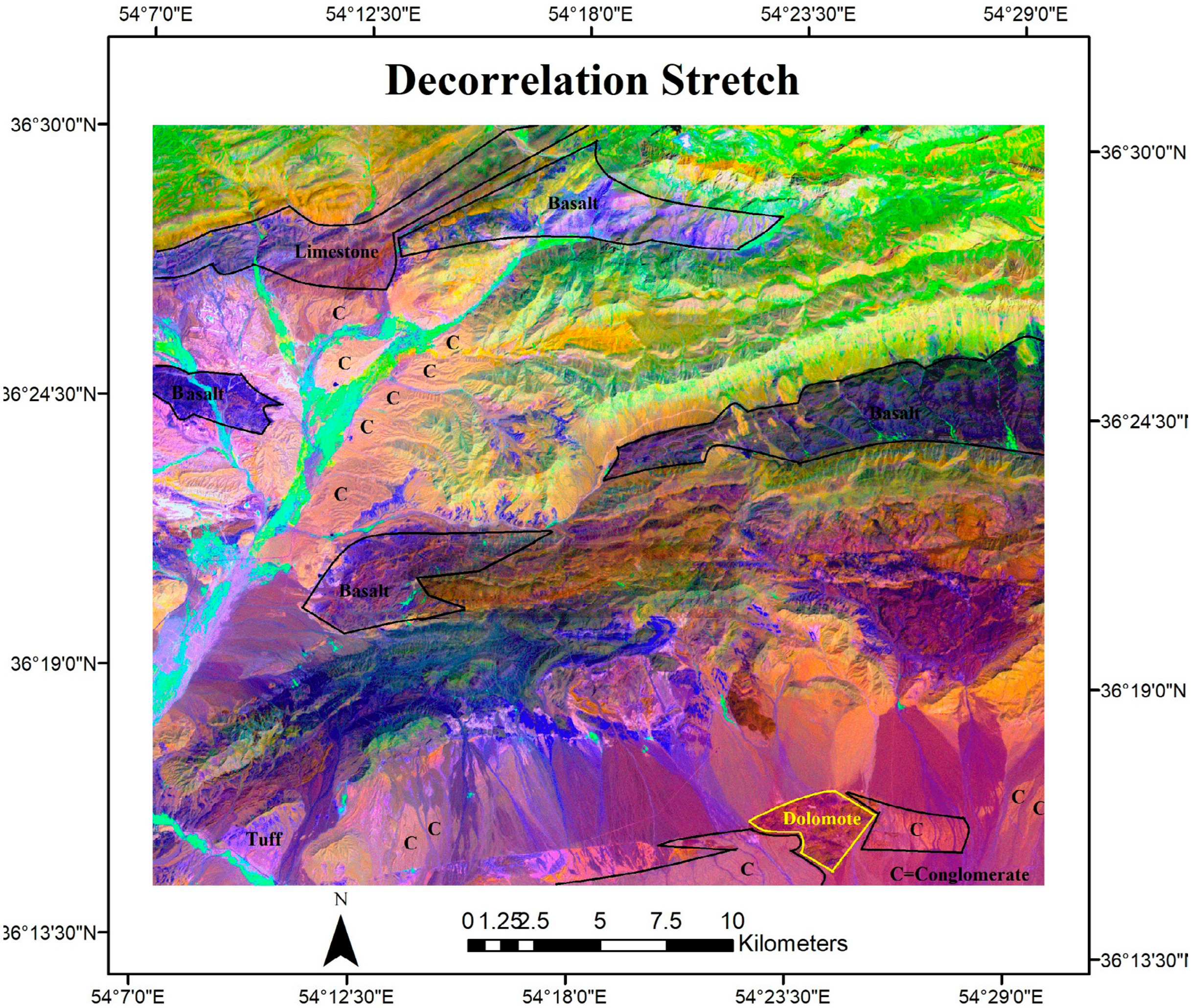


Figure 5. Decorrelation stretch output

the study of Aali et al. (2022), suitability of the PCA and BR techniques was demonstrated for detection of the geological units such as Sandstone, Dolomite, Conglomerate, Limestone and Marl in the Chakchak region, Yazd province, Iran. Pournamdari et al. (2014) also proved applicability of these techniques for lithological mapping of Soghan ophiolitic complex in south of Iran. Aboelkhair and Watanabe (2011) sucsessgully performed the PCA and DS techniques for mapping Basalt flow in Madinah area, Saudi Arabia. Moreover, Sekandari et al. (2020) executed the PCA, MNF and BR techniques for the extraction of lithological units such as Dolomite, Limestone, Basalt, Sandstone, Conglomerate and Tuff in the central part of the Kashmar–Kerman tectonic zone, the Central Iranian Terrane (CIT). Similarly, in the study of Othman and Gloaguen (2017), the applicability of PCA, BR and classification techniques was verified for mapping the geological units such as Conglomerate, Limestone, Tuff and reddish green Shales in the Bardi-Zard area in north-east Iraq, a part of the Zagros Fold – Thrust Belt. As shown in the above studies, the principal component analysis and band ratio were the most widely used techniques for geological mapping using satellite data.

## 4. CONCLUSION

In this study, the applicability of several image processing techniques, including the band ratio (BR), decorrelation stretch (DS), principal components anal-

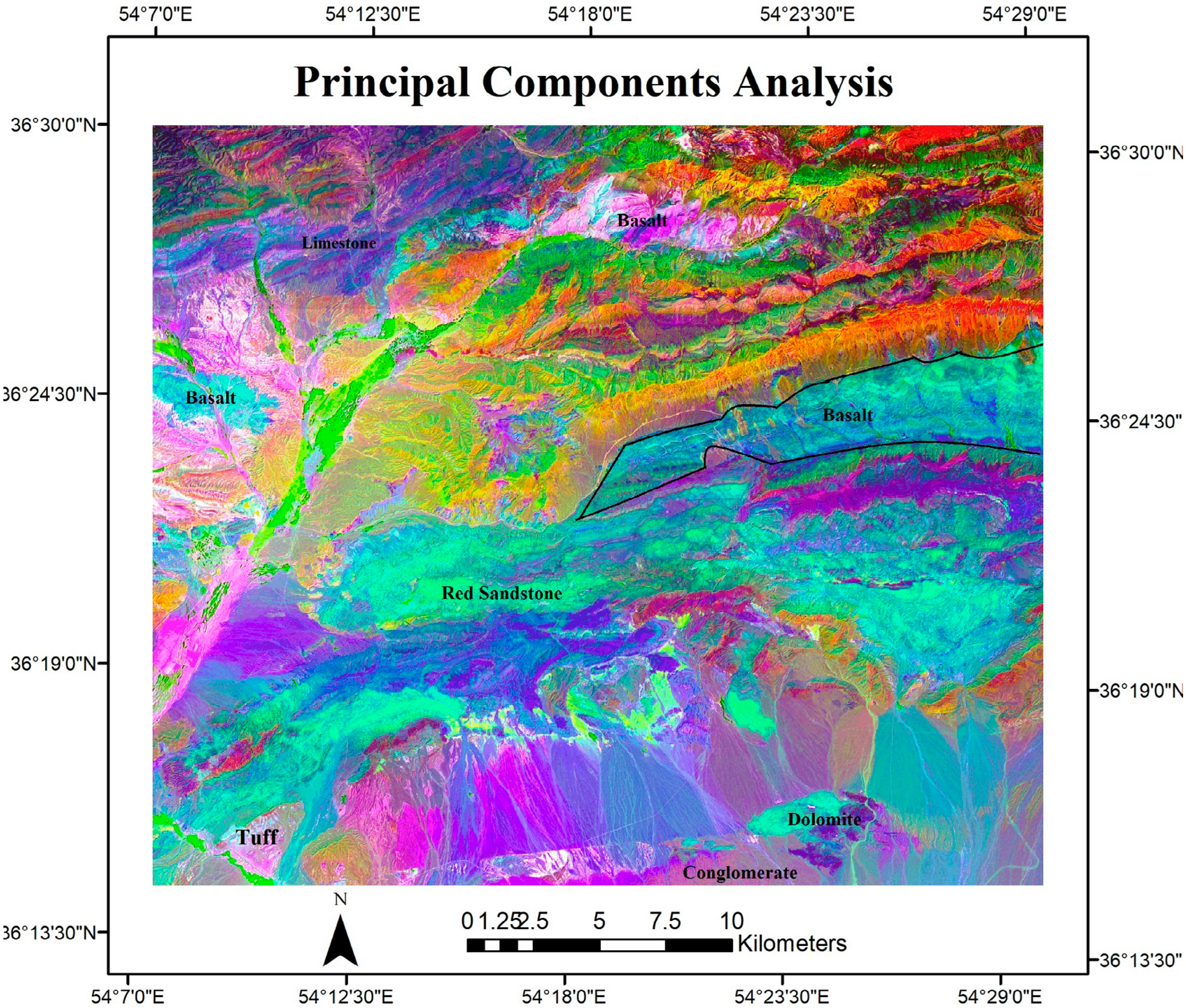


FIGURE 6. PRINCIPAL COMPONENTS ANALYSIS (PC1, PC2, PC3 AS RGB)

ysis (PCA), minimum noise fraction (MNF), and the ASTER false color composition RGB: 468, was evaluated for the extraction of geological units from ASTER satellite imagery in southern margin of Alborz Mountain in Iran. In addition, a method based on Principal Components of Band Ratios (BRs-PCs) was proposed for the discrimination of geological units from ASTER imagery. The results indicated that the ASTER RGB:468 and MNF technique were not able to clearly highlight Limestone and Basalt from ASTER image, while the DS technique successfully discriminated all the geological units except for Sandstone. In addition, the results revealed that the specified band ratios could not extract Limestone from ASTER image. In contrast, PCA technique highlighted all the geological units in the study area, however a failure was appeared in discrimination of Basalt using this technique. Nonetheless, the BRs-PCs approach, because considered the advantages of both PCA and BR techniques, provided a superior output compared to these techniques alone, and successfully discriminated all the geological units from ASTER imagery. The study concluded that the BRs-PCs approach may be useful for geological mapping along the whole Alborz Mountain with similar lithological and geomorphological conditions.

## ACKNOWLEDGMENTS

This work was supported by Gonbad Kavous University through Grant No: 6/567.

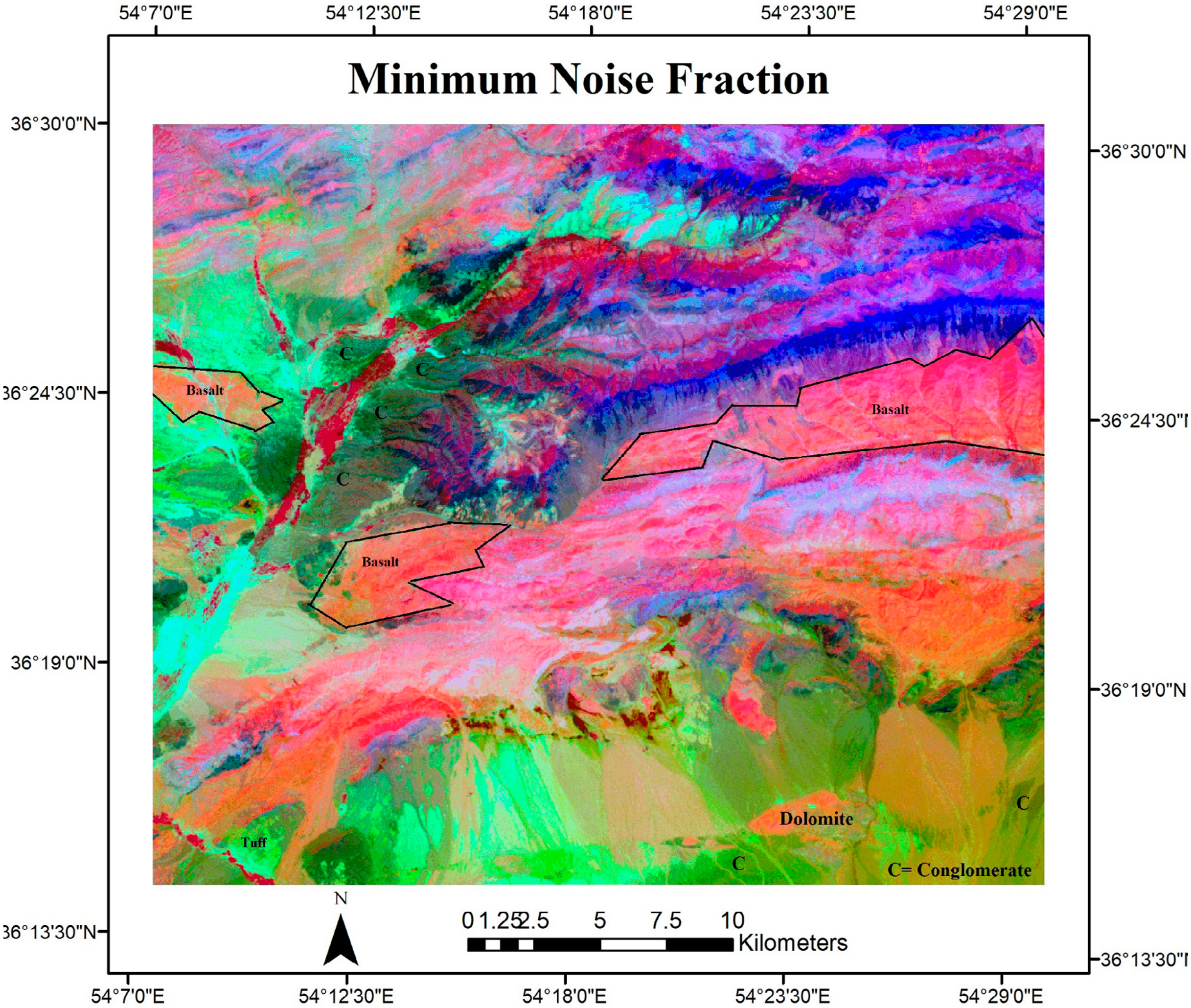


Figure 7. Minimum noise fraction result

## DECLARATIONS

The authors declare no conflict of interest.

## DECLARATION OF AUTHORSHIP CONTRIBUTION

Komeil Rokni developed the methodology, analyzed the data, and prepared the manuscript. Davood Akbari provided critical feedback in data analysis and contributed to the final manuscript

## REFERENCES

Aali, A. A., Shirazy, A., Shirazi, A., Pour, A. B., Hezarkhani, A., Maghsoudi, A., and Khakmardan, S. (2022). Fusion of remote sensing, magnetometric, and geological data to identify polymetallic mineral potential zones in Chakchak Region, Yazd, Iran. *Remote Sensing*, *14*(23), 6018. https://doi.org/10.3390/rs14236018.

Abdelouhed, F., Ahmed, A., Abdellah, A., Mohammed, I., & Zouhair, O. (2021). Extraction and analysis of geological lineaments by combining ASTER-GDEM and Landsat 8 image data in the central high atlas of Morocco. *Natural Hazards*, *111(2)*, 1907-1929. https://doi.org/10.1007/s11069-021-05122-9.

Aboelkhair, H., & Watanabe, Y. (2011). Using remotely sensed multispectral ASTER data for mapping extensive basalt flow around Al Madinah area, Saudi Arabia. In *First International Geomatics*

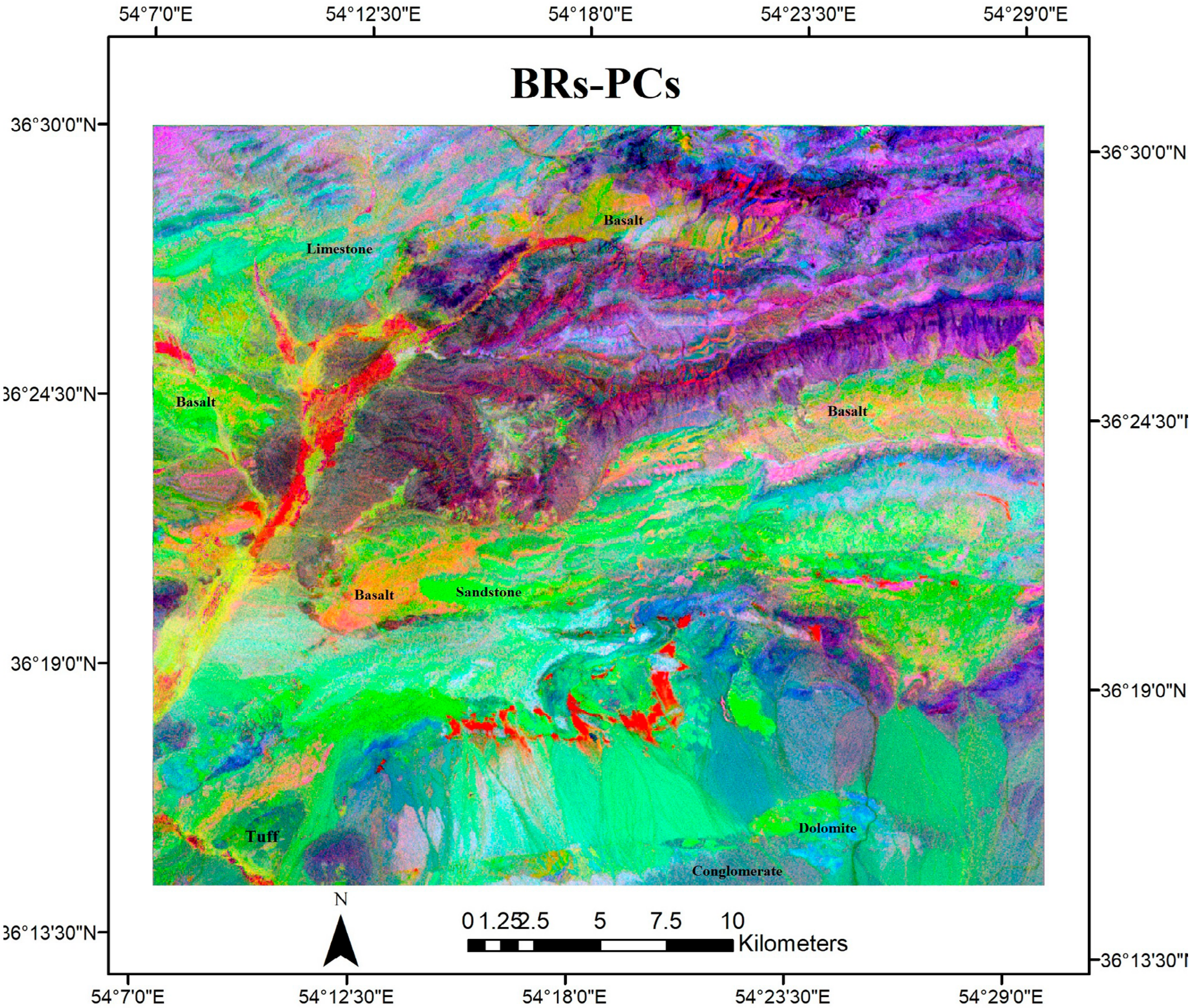


FIGURE 8. BRS-PCS (BRS-PC1, BRS-PC2, BRS-PC3 AS RGB)


*Symposium in Saudi Arabia, Geomatics Technologies in the City, GTC*. https://doi.org/10.13140/RG.2.1.1756.8802.

Adams, J. B., and Filice, A. L. (1967). Spectral reflectance 0.4 to 2.0 microns of silicate rock powders. *Journal of Geophysical Research*, *72*(22), 5705-5715. https://doi.org/10.1029/JZ072i022p05705.

Amer, R., Kusky, T., and Ghulam, A. (2010). Lithological mapping in the Central Eastern Desert of Egypt using ASTER data. *Journal of African Earth Sciences*, *56*(2-3), 75-82. https://doi.org/10.1016/j.jafrearsci.2009.06.004.

Arabameri, A., Roy, J., Saha, S., Blaschke, T., Ghorbanzadeh, O., and Tien Bui, D. (2019). Application of probabilistic and machine learning models for groundwater potentiality mapping in Damghan sedimentary plain, Iran. *Remote Sensing*, *11*(24), 1-35. https://doi.org/10.3390/rs11243015.

Bernknopf, R. L. (1993). *Societal value of geologic maps* (Vol. 1111). DIANE Publishing.

Bhan, S. K., & Krishnanunni, K. (1983). Applications of remote sensing techniques to geology. *Proceedings of the Indian Academy of Sciences Section C: Engineering Sciences*, *6*, 297-311.

Compton, R. R., and Compton, R. R. (1985). *Geology in the Field* (p. 416). New York: Wiley.

Davis, G. H., Reynolds, S. J., and Kluth, C. F. (2011). *Structural geology of rocks and regions*. John Wiley & Sons.

Fal, S., Maanan, M., Baidder, L., and Rhinane, H. (2019). The contribution of Sentinel-2 satellite images for geological mapping in the south of Tafilalet basin (Eastern Anti-Atlas, Morocco). *The International Archives of the Photogrammetry, Remote Sensing and Spatial Information Sciences*, *42*, 75-82. https://doi.org/10.5194/isprs-archives-XLII-4-W12-75-2019.

Gabr, S., Ghulam, A., and Kusky, T. (2010). Detecting areas of high-potential gold mineralization using ASTER data. *Ore Geology Reviews*, *38*(1-2), 59-69. https://doi.org/10.1016/j.oregeorev.2010.05.007.

Gillespie, A., Rokugawa, S., Matsunaga, T., Cothern, J. S., Hook, S., and Kahle, A. B. (1998). A temperature and emissivity separation algorithm for Advanced Spaceborne Thermal Emission and Reflection Radiometer (ASTER) images. *IEEE transactions on geoscience and remote sensing*, *36*(4), 1113-1126. https://doi.org/10.1109/36.700995.

Green, A. A., Berman, M., Switzer, P., and Craig, M. D. (1988). A transformation for ordering multispectral data in terms of image quality with implications for noise removal. *IEEE Transactions on geoscience and remote sensing*, *26*(1), 65-74. https://doi.org/10.1109/36.3001.

Hewson, R. D., Cudahy, T. J., Mizuhiko, S., Ueda, K., and Mauger, A. J. (2005). Seamless geological map generation using ASTER in the Broken Hill-Curnamona province of Australia. *Remote Sensing of Environment*, *99*(1-2), 159-172. https://doi.org/10.1016/j.rse.2005.04.025.

Hewson, R., Robson, D., Carlton, A., and Gilmore, P. (2017). Geological application of ASTER remote sensing within sparsely outcropping terrain, Central New South Wales, Australia. *Cogent Geoscience*, *3*(1), 1319259. https://doi.org/10.1080/23312041.2017.1319259.

Hook, S. J., Gabell, A. R., Green, A. A., and Kealy, P. S. (1992). A comparison of techniques for extracting emissivity information from thermal infrared data for geologic studies. *Remote Sensing of Environment*, *42*(2), 123-135. https://doi.org/10.1016/0034-4257(92)90096-3.

Inzana, J., Kusky, T., Higgs, G., and Tucker, R. (2003). Supervised classifications of Landsat TM band ratio images and Landsat TM band ratio image with radar for geological interpretations of central Madagascar. *Journal of African Earth Sciences*, *37*(1-2), 59-72. https://doi.org/10.1016/S0899-5362(03)00071-X.

Kenea, N. H. (1997). Improved geological mapping using Landsat TM data, Southern Red Sea Hills, Sudan: PC and IHS decorrelation stretching. *International Journal of Remote Sensing*, *18*(6), 1233-1244. https://doi.org/10.1080/014311697218386.

Khan, S. D., Mahmood, K., and Casey, J. F. (2007). Mapping of Muslim Bagh ophiolite complex (Pakistan) using new remote sensing, and field data. *Journal of Asian Earth Sciences*, *30*(2), 333-343. https://doi.org/10.1016/j.jseaes.2006.11.001.

Kühn, J., Brenning, A., Wehrhan, M., Koszinski, S., and Sommer, M. (2009). Interpretation of electrical conductivity patterns by soil properties and geological maps for precision agriculture. *Precision Agriculture*, *10*(6), 490-507. https://doi.org/10.1007/s11119-008-9103-z.

Loughlin, W. P. (1991). Principal component analysis for alteration mapping. *Photogrammetric Engineering and Remote Sensing*, *57*(9), 1163-1169.

NASA, L. D. (2021). ASTER level 1 precision terrain corrected registered at-sensor radiance V003 [data set]. *NASA EOSDIS land processes DAAC.*

Ninomiya, Y., Fu, B., and Cudahy, T. J. (2005). Detecting lithology with Advanced Spaceborne Thermal Emission and Reflection Radiometer (ASTER) multispectral thermal infrared "radiance-at-sensor" data. *Remote Sensing of Environment*, *99*(1-2), 127-139. https://doi.org/10.1016/j.rse.2005.06.009.

Othman, A. A., and Gloaguen, R. (2017). Integration of spectral, spatial and morphometric data into lithological mapping: A comparison of different Machine Learning Algorithms in the Kurdistan Region, NE Iraq. *Journal of Asian Earth Sciences*, *146*, 90-102. https://doi.org/10.1016/j.jseaes.2017.05.005.

Pournamdari, M., Hashim, M., and Pour, A. B. (2014). Spectral transformation of ASTER and Landsat TM bands for lithological mapping of Soghan ophiolite complex, south Iran. *Advances in Space Research*, *54*(4), 694-709. https://doi.org/10.1016/j.asr.2014.04.022.

Pour, A. B., and Hashim, M. (2015). Structural mapping using PALSAR data in the central gold belt, Peninsular Malaysia. *Ore Geology Reviews*, *64*, 13-22. https://doi.org/10.1016/j.oregeorev.2014.06.011.

Prost, G. L. (2013). *Remote sensing for geoscientists: image analysis and integration*. New York: CRC Press.

Rezaei, A., Hassani, H., Moarefvand, P., and Golmohammadi, A. (2020). Lithological mapping in Sangan region in Northeast Iran using ASTER satellite data and image processing methods. *Geology, Ecology, and Landscapes*, *4*(1), 59-70. https://doi.org/10.1080/24749508.2019.1585657.

Rokni, K., Marghany, M., Hashim, M., and Hazini, S. (2011, December). Performance evaluation of global and absolute DEMs generated from ASTER stereo imagery. In *2011 IEEE International RF & Microwave Conference* (pp. 266-269). https://doi.org/10.1109/RFM.2011.6168745.

Sekandari, M., Masoumi, I., Beiranvand Pour, A., M Muslim, A., Rahmani, O., Hashim, M., and Aminpour, S. M. (2020). Application of Landsat-8, Sentinel-2, ASTER and WorldView-3 spectral imagery for exploration of carbonate-hosted Pb-Zn deposits in the Central Iranian Terrane (CIT). *Remote Sensing*, *12*(8), 1239. https://doi.org/10.3390/rs12081239.

Seleem, T., Hamimi, Z., Zaky, K., and Zoheir, B. (2020). ASTER mapping and geochemical analysis of chromitite bodies in the Abu Dahr ophiolites, South Eastern Desert, Egypt. *Arabian Journal of Geosciences*, *13*, 1-21. https://doi.org/10.1007/s12517-020-05624-z.

Soller, D. R. (Ed.). (2002). *Digital Mapping Techniques' 02, Workshop Proceedings: May 19-22, 2002, Salt Lake City, Utah* (Vol. 2, No. 370). US Department of the Interior, US Geological Survey.

Sultan, M., Arvidson, R. E., and Sturchio, N. C. (1986). Mapping of serpentinites in the Eastern Desert of Egypt by using Landsat thematic mapper data. *Geology*, *14*(12), 995-999. https://doi.org/10.1130/0091-7613(1986)14<995:MOSITE>2.0.CO;2.

Ullmann, T., Büdel, C., Baumhauer, R., and Padashi, M. (2016). Sentinel-1 SAR data revealing fluvial morphodynamics in damghan (Iran): Amplitude and coherence change detection. *International Journal of Earth Science and Geophysics*, *2*(1), 1-14. https://doi.org/10.35840/2631-5033/1807.

Varnes, D. J. (1974). The logic of geological maps, with reference to their interpretation and use for engineering purposes. USGS Professional Paper 837.

Yang, M., Ren, G., Han, L., Yi, H., and Gao, T. (2018). Detection of Pb–Zn mineralization zones in west Kunlun using Landsat 8 and ASTER remote sensing data. *Journal of Applied Remote Sensing*, *12*(2), 026018-026018. https://doi.org/10.1117/1.JRS.12.026018.